Rapid Communications

Enhanced dynamics in fusion of neutron-rich oxygen nuclei at above-barrier energies

S. Hudan and R. T. deSouza*
Department of Chemistry and Center for Exploration of Energy and Matter, Indiana University, 2401 Milo B. Sampson Lane, Bloomington, Indiana 47408, USA

A. S. Umar
Department of Physics and Astronomy, Vanderbilt University Nashville, Tennessee 37235, USA

Z. Lin
Department of Physics and Center for Exploration of Energy and Matter, Indiana University, 2401 Milo B. Sampson Lane, Bloomington, Indiana 47408, USA and Department of Physics, Arizona State University, 450 E. Tyler Mall, Tempe, Arizona 85287-1504, USA

C. J. Horowitz
Department of Physics and Center for Exploration of Energy and Matter, Indiana University, 2401 Milo B. Sampson Lane, Bloomington, Indiana 47408, USA

(Received 31 March 2020; revised manuscript received 20 April 2020; accepted 26 May 2020; published 11 June 2020)

Above-barrier fusion cross sections for an isotopic chain of oxygen isotopes with $A = 16$–19 incident on a ^{12}C target are presented. Experimental data are compared with both static and dynamical microscopic calculations. These calculations are unable to explain the ≈37% increase in the average above-barrier fusion cross section observed for ^{19}O as compared to β-stable oxygen isotopes. This result suggests that for neutron-rich nuclei existing time-dependent Hartree-Fock calculations underpredict the role of dynamics at near-barrier energies. High-quality measurement of above-barrier fusion for an isotopic chain of increasingly neutron-rich nuclei provides an effective means to probe this fusion dynamics.

DOI: 10.1103/PhysRevC.101.061601

Nuclei with an exotic neutron-to-proton ratio provide a unique opportunity to test our microscopic understanding of nuclei. A distinguishing characteristic of these nuclei is the difference in the spatial extent of their neutron and proton density distributions. By systematically comparing nuclei along an isotopic chain one can gain insight into the evolution of nuclear properties with neutron number. This approach resulted in the discovery of the halo nature of ^{11}Li [1]. To date, considerable effort has been expended to understand ground-state properties, e.g., size, shape, two neutron separation energies, pairing correlations, etc., of these exotic nuclei [2–5]. As neutron-rich nuclei play a key role in r-process nucleosynthesis reactions [6], it is crucial to understand not only their ground state properties but the response of these weakly bound systems to perturbation. Fusion reactions provide a powerful means to assess the response of neutron-rich nuclei to perturbation. As fusion involves the interplay of the repulsive Coulomb and attractive nuclear potentials, by examining fusion for an isotopic chain one probes the neutron density distribution and how that density distribution evolves as the two nuclei approach and overlap [7,8]. Fusion of neutron-rich nuclei has also been hypothesized as providing a heat source that triggers an x-ray superburst in an accreting neutron star [9]. Investigating the fusion of neutron-rich nuclei is thus also important for understanding such astrophysical events. Radioactive beam facilities, both those in existence [10–12] as well as those on the horizon [13] make such measurements feasible for the first time.

In the present work we examine the dependence of the above-barrier fusion cross section for ^{16,17,18,19}O ions on a ^{12}C target. As only above-barrier energies will be experimentally accessible for the most neutron-rich beams, it is important to assess how sensitively changes in neutron number impact the fusion cross section in this energy regime. This above-barrier cross section can be related to an interaction radius at which the projectile and target nuclei fuse, i.e., the dynamical size of the system as it fuses. Comparison of fusion at near and sub-barrier energies for a wide variety of projectile/target combinations has typically resorted to a scaling approach to disentangle static and dynamic contributions [14]. By focusing on an isotopic chain incident on a single target nucleus the need for such scaling is minimized. In this work, the static and dynamic contributions to the above-barrier fusion cross section are disentangled through direct comparison of

*desouza@indiana.edu

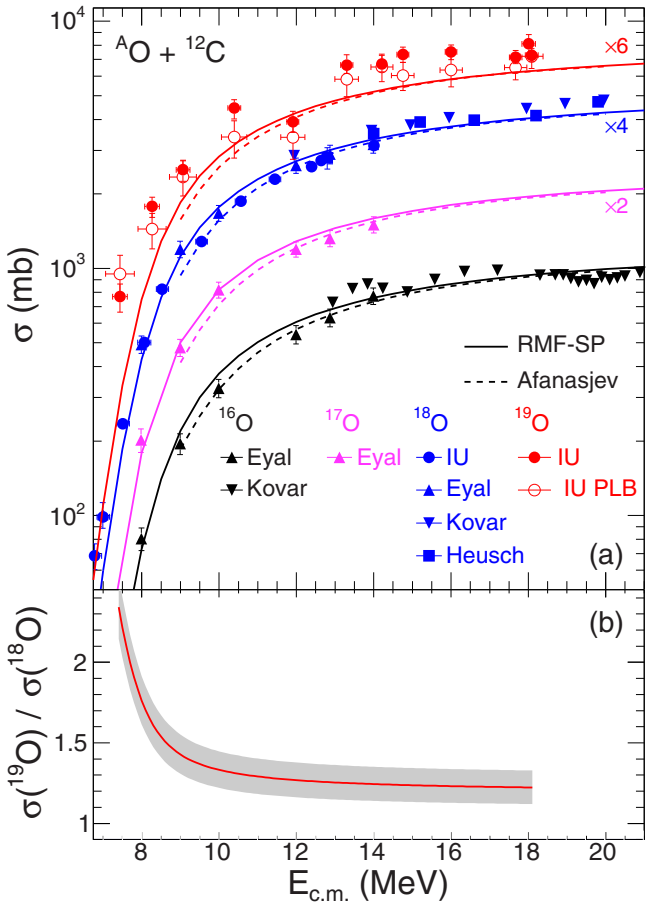

FIG. 1. Top panel: Fusion excitation functions for ^{16,17,18,19}O + ^{12}C (symbols) are presented along with the calculations of the RMF-SP model (solid lines). The predictions of an analytic fusion model [15] are indicated by the dashed lines. For clarity, both data and calculations have been scaled by the factors shown. Bottom panel: Ratio of the fusion cross-section ^{19}O/^{18}O. See text for details.

the experimental results with the predictions of different microscopic models.

Presented in Fig. 1(a) are the fusion excitation functions for ^{16,17,18,19}O ions on a ^{12}C target. The data for the ^{16,17,18}O induced reactions have been taken from the literature [16–18] and in the case of ^{18}O supplemented by our prior measurement [19]. All the excitation functions shown are relatively flat at higher energies and at lower energies fall exponentially with decreasing energy signaling a barrier-driven process. In addition to the overall characteristic shape, one observes for ^{16}O + ^{12}C a clear increase in the cross section in the interval 12 MeV $< E_{c.m.} <$ 18 MeV. Precision measurements in this energy regime associate this increased cross section with well-known resonances [20]. Resonances in the case of the other oxygen isotopes are not as discernible.

In addition to the fusion excitation function for the β-stable nuclei, the fusion excitation function for ^{19}O + ^{12}C is also shown in Fig. 1(a). Although these cross sections had been previously reported [7], an improved calibration has allowed a two- to fourfold improvement in the statistical quality of the data presented [21]. Identification of heavy fusion products was accomplished through use of an energy/time-of-flight approach [19] with the heavy products detected in annular, double-sided silicon detectors. The new calibration of the silicon detectors allowed inclusion of heavy fusion products over a wider azimuthal range than previously reported. In these detectors, for each incident particle, electrons and holes were independently collected. To ensure correct identification of a heavy fusion product, it was required that the energy associated with both holes and electrons agree to within ±0.5 MeV. The improved energy calibration has resulted in the reduction of the number of particles rejected by this energy constraint. The reanalyzed cross section for ^{18}O + ^{12}C measured simultaneously agrees with the published cross sections [7] within the statistical uncertainties.

The original and the revised cross sections are presented as the open red circles and closed red circles, respectively. The revised cross sections are approximately 14% larger than those previously published [7]. A few points are noteworthy about the new results. With the exception of the lowest energy, the revised cross sections are consistently larger than those originally reported although the new cross sections typically lie within the uncertainties previously reported. The reduction in the uncertainty of the fusion cross section with the improved statistics is significant. For the the lowest energy point the cross section decreases from 158 mb to 128 mb. Inspection of the cross section in Fig. 1(a) reveals that typical cross section above the barrier for ^{19}O is ≈ 1200 mb whereas for ^{18}O and ^{16}O it is ≈1000 mb. It should be emphasized that the magnitude of this increase in the cross-section is robustly measured as a simultaneous measurement of ^{18,19}O + ^{12}C was performed [7].

The impact of changes in the nuclear size on the fusion cross section, absent any dynamics, was assessed by employing the São Paulo model [22] to predict the fusion cross section. The frozen density distributions were determined using a relativistic mean field (RMF) approach using the FSUGOLD interaction [23,24]. The results of these calculations, designated RMF-SP, are presented in Fig. 1 as solid lines. While the predictions of the RMF-SP model is in reasonable agreement with the experimental cross sections for ^{16}O and ^{18}O (and the limited existing data for ^{17}O), in the case of ^{19}O the RMF-SP model systematically underpredicts the measured cross sections.

We have also compared the measured excitation functions with the predictions of an analytical model based on a parametrization of the Sao Paulo potential model coupled with a barrier penetration formalism [15,25,26]. This model which has parametrized a large number of reactions is a useful tool for network simulations. The above-barrier cross sections predicted by this model are depicted in Fig. 1(a) as the dashed lines. The cross sections from the analytic model lie close to the RMF-SP values but are slightly smaller in magnitude. While providing a reasonable description of the ^{16,17,18}O data, the analytical fusion model also underpredicts the ^{19}O excitation function.

To examine this enhancement of the fusion cross section for ^{19}O more quantitatively and with less sensitivity to systematic uncertainties, the ratio of $\sigma(^{19}\mathrm{O})/\sigma(^{18}\mathrm{O})$ is also presented in Fig. 1(b). To construct this ratio the

TABLE I. Woods-Saxon parameters used in the CCFULL calculations for the different systems.

	V_C (MeV)	r_0 (fm)	a (fm)
$^{16}O+^{12}C$	−256.0	0.770	0.720
$^{17}O+^{12}C$	−256.0	0.770	0.720
$^{18}O+^{12}C$	−281.0	0.741	0.759
$^{19}O+^{12}C$	−300.0	0.740	0.759

experimental excitation functions have been fit with a simple barrier penetration formalism [7,27]. In the above-barrier regime the ratio is relatively flat with a value of approximately 1.22. The uncertainty in the ratio is depicted by the shaded region.

Given the underprediction of the measured cross section by the static RMF-SP calculation for ^{19}O, the role of dynamics was considered. A coupled channels approach [28] was utilized to assess the impact of dynamics on the fusion cross section. Coupled channels calculations consider fusion dynamics as the coupling to excited states of the colliding nuclei through mutual Coulomb excitation. Calculations with this coupled-channel approach have been successful at describing the fusion of stable and near β-stable nuclei [29]. Calculations were performed with the coupled channels code CCFULL [30] using the Woods-Saxon potential parameters listed in Table I. The value for these parameters was chosen consistent with the Akyuz-Winther optical model and based on elastic scattering data [31]. For ^{12}C, vibrational coupling to the 2^+ state at 4.439 MeV was included. In the case of ^{16}O and ^{18}O, vibrational coupling to the 2^+ state at 6.917 MeV and 1.982 MeV was accounted for while for ^{17}O and ^{19}O, rotational coupling to the excited state at 8.466 MeV and 2.779 MeV, respectively, a $\frac{7}{2}^+$ state, was included. The resulting fusion excitation functions for the various oxygen isotopes are shown in Fig. 2 as solid lines. The overall description of the measured fusion excitation functions is reasonable with the exception of ^{19}O. In this case, in order to obtain a reasonable description of the excitation function it was necessary to increase the radius parameter in the Woods-Saxon potential from 0.74 fm to 0.85 fm. The result of the latter calculation is represented by the long dashed line. The need to arbitrarily increase the radius parameter by 15% in order to reproduce the measured cross sections could be interpreted as the contribution of additional excited states to the fusion cross section.

To provide an independent assessment of the role of dynamics while avoiding the arbitrary truncation at a finite number of excited states, we chose to compare the experimental data with the predictions of a time-dependent Hartree-Fock (TDHF) model. On general grounds a TDHF approach is well suited to describing the large-amplitude collective motion associated with fusion. Recently, advances in theoretical and computational techniques allow TDHF calculations to be performed on a three-dimensional (3D) Cartesian grid thus eliminating artificial symmetry restrictions [32]. While in the subbarrier regime in order to accurately describe the fusion cross-sections it is necessary to perform density constrained TDHF

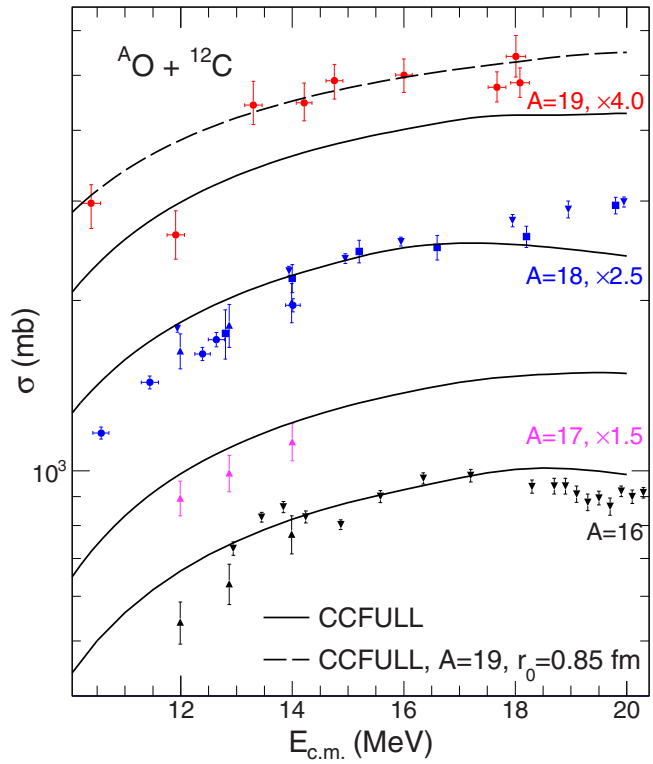

FIG. 2. Comparison of CCFULL calculations (solid lines) with the experimental excitation functions. The long dashed line depicts the CCFULL calculations using a radius parameter of $r_0 = 0.85$ fm for ^{19}O. Both data and calculations are scaled by the factors indicated for clarity.

(DC-TDHF) calculations [19,33,34] to obtain the heavy-ion potentials [35], at the above-barrier energies considered in this work direct TDHF calculations can be performed by initiating collisions for increasing impact parameters until the maximum impact parameter for fusion is reached. In practice this was done with an impact parameter precision of 0.02 fm. For odd nuclei frozen pairing approximation was used in TDHF calculations.

A self-consistent reference point for the TDHF calculations is provided by first calculating the cross section by folding frozen Hartree-Fock density distributions (FHF). As they lack the nonlocal character present in the RMF, these density distributions are slightly different from the density distributions used in the RMF-SP calculation. Consequently, the fusion cross sections predicted by the FHF model are slightly larger than those predicted by the RMF-SP. The predictions of the FHF model (dashed line) are compared with the experimental data in Fig. 3. In the case of ^{16,17,18}O the predicted fusion cross section matches or slightly exceeds the experimental cross sections. For ^{19}O however, the predicted cross sections underpredict the experimental values. The impact of the dynamics on the cross section is indicated by the difference between the FHF calculations and the TDHF results (solid line). While the impact of the dynamics for these systems is not large, as expected, inclusion of dynamics acts to increase the predicted cross sections. Even with this inclusion of dynamics,

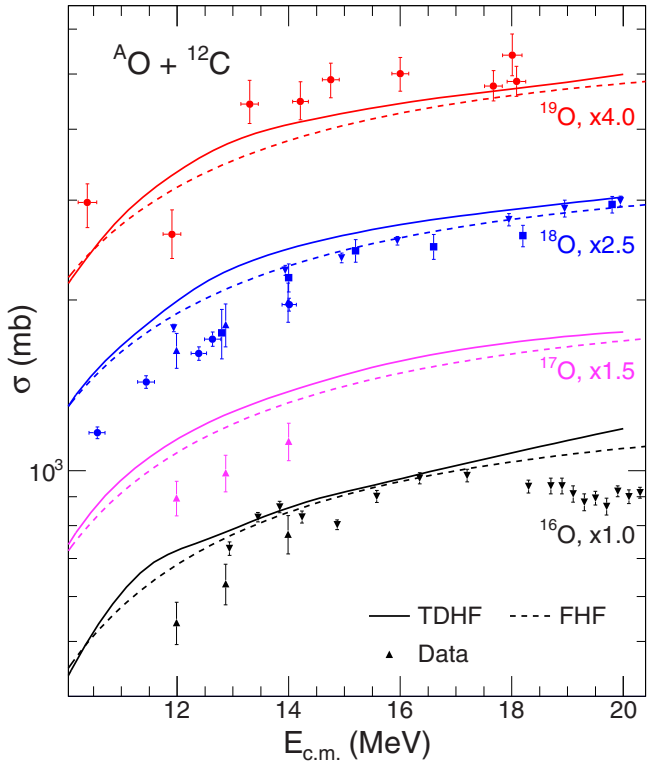

FIG. 3. Comparison of TDHF and FHF calculations with the experimental excitation functions. Both data and calculations are scaled by the factors indicated for clarity.

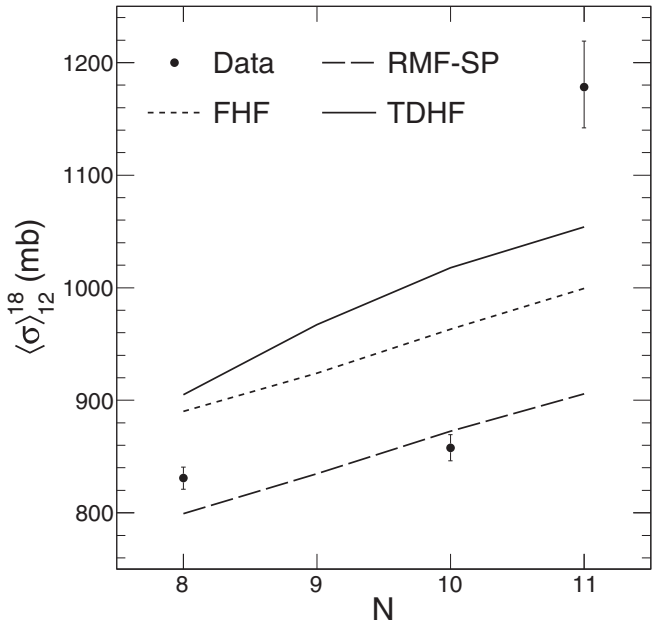

FIG. 4. Dependence of the average fusion cross-section in the interval 12 MeV $< E_{c.m.} <$ 18 MeV on neutron number. Experimental cross sections are compared with the results of calculations with the RMF-SP, FHF, and TDHF models.

however, the measured cross sections for fusion of $^{19}O + ^{12}C$ are underpredicted. This is particularly surprising since for light systems, due to the absence of breakup, the TDHF usually overpredicts the fusion cross sections. The relatively small difference between the FHF and TDHF calculations suggests that normally considered excitations of the entrance channel nuclei are unlikely to play a significant role at above barrier energies for light nuclei. This result also suggests that the enhancement in the fusion cross section for ^{19}O is *not* a standard excitation.

The dependence of the average fusion cross section on neutron number is examined in Fig. 4. The quantity $< \sigma >_{12}^{18}$ represents the average fusion cross section determined over the range 12 MeV $< E_{c.m.} <$ 18 MeV. While the average cross section for ^{16}O and ^{18}O is comparable, 831 mb and 858 mb, respectively, ^{19}O manifests a significantly higher cross section of 1178 mb. This corresponds to a ≈37% increase in cross section with the addition of a single neutron to ^{18}O. This ≈37% increase in the experimental above-barrier fusion cross section with the addition of a single neutron is remarkable. It should be compared to the increase of the total cross section in the case of the Li isotopes [36]. For the halo nucleus ^{11}Li, the total reaction cross section increases by 30% as compared to ^{9}Li, a comparable increase. This increase in the cross section for the addition of two neutrons is associated with an increase in the interaction radius from ≈2.4 fm (^{9}Li) to ≈3.2 fm (^{11}Li) [1]. It should be appreciated however that the high-energy measurement of the total reaction cross section probes effectively the static size of the nuclei. In contrast, the near-barrier fusion cross section presented in this work reflects both the static and dynamic contributions to the size of the fusing system. The measured interaction cross section for ^{18,19}O on a carbon target at ≈ 900A MeV [37] exhibits only a modest increase from 1032 ± 26 mb to 1066 ± 9 mb with increasing neutron number. This result directly indicates that the measured increase in the near-barrier fusion cross section is not the result of simply a larger static size or deformation but results from the low-energy fusion dynamics. Although the quantity $< \sigma >_{12}^{18}$ cannot be calculated for ^{17}O due to the lack of experimental data, it can be estimated from Fig. 1(a) that if the data followed the smooth behavior predicted by the RMF-SP model, one would expect that $< \sigma >_{12}^{18}$ would have a value of ≈ 820 mb. This suggests that the fusion enhancement for ^{19}O is not due to an odd even effect. This expectation requires experimental verification.

The impact of breakup on the fusion cross section is a natural question to consider as the projectile nuclei become more weakly bound with increasing neutron number. In the case of $^{11}Li + ^{208}Pb$, the fusion cross section predicted by the TDHF model exceeded the measured cross section [38]. Other models provided a similar overprediction [38]. This overprediction was attributed to the absence of breakup processes in the TDHF model prior to fusion. Projectile breakup is induced either by the target's Coulomb field or its nuclear field. For Coulomb-driven breakup the breakup probability is expected to scale with atomic number [39]. Given the low atomic number of the target nucleus in these reactions it is expected that any breakup is dominantly nuclear [40]. Given the range of the nuclear force, this breakup occurs when the two nuclei are close, leading to a higher probability

of capture. Consideration of the Q values for the nuclei under consideration argues against a dramatic change in the role of breakup for ^{19}O. The Q value of single neutron removal for $^{19}\mathrm{O} \rightarrow {}^{18}\mathrm{O}+n$ is -3.96 MeV, comparable to is -4.14 MeV for $^{17}\mathrm{O} \rightarrow {}^{16}\mathrm{O}+n$. Two-neutron removal for $^{19}\mathrm{O} \rightarrow {}^{17}\mathrm{O}+2n$ is -12.00 MeV, very comparable to the $Q_{2n} = -12.19$ MeV for ^{18}O. Thus, based on the Q values a significant change in the role of capture following neutron breakup is not expected.

The predictions of the average cross-section for the RMF-SP, FHF, and TDHF models are indicated by the dashed, dotted, and solid lines, respectively. The RMF-SP and FHF exhibit a similar slope with the RMF-SP systematically predicting a smaller cross section (smaller interaction radius) than the FHF model. Although the RMF-SP is in better agreement with the experimental data for ^{16,18}O, neither the FHF nor the RMF-SP provides an adequate description of the ^{19}O cross section. The better agreement between the RMF-SP model and the experimental data for ^{16,18}O may be due to its inclusion of momentum correlations between the nucleons, which presumably results in more accurate density distributions than the FHF model. From the comparison of the RMF-SP with the ^{19}O cross section it is clear that ^{19}O nucleus does not follow the simple scaling due to nuclear size as incorporated into the RMF model. The TDHF model which includes dynamics predicts a slightly larger cross-section than the FHF model with a slightly stronger dependence on neutron number. However, the TDHF model still fails to describe the measured cross section for ^{19}O. The difference between the TDHF and FHF calculations indicates the degree to which dynamics, *as realized in the TDHF model*, impacts the fusion cross section at above-barrier energies.

Comparison of the experimental data with the static RMF-SP and FHF models demonstrates that while the cross sections for ^{16}O and ^{18}O can be understood as primarily due to the static size of the nuclei, the enhancement of the fusion cross section for ^{19}O significantly exceeds the prediction of these static models. Even inclusion of dynamics with the TDHF model is insufficient to explain the increase. This underprediction of experimental cross sections by TDHF also implies that substantially expanding the number of excited states included in the CCFULL model would also underpredict the experimental data.

The underprediction of the experimental fusion cross sections by the TDHF model suggests that extremely large-amplitude collective motion are not sufficiently represented in the TDHF model. Though they may be rare, these extremely large-amplitude deformations may play a crucial role in the fusion process. Whether these large-amplitude deformations are coupled to bound states or the continuum is presently unclear. What is clear is that high-quality measurement of above-barrier fusion for an isotopic chain of increasingly neutron-rich nuclei provides an effective means to probe these deformations, underscoring the importance of such measurements for the most neutron-rich light nuclei accessible.

This work was supported by the U.S. Department of Energy under Grant No. DE-FG02-88ER-40404 (Indiana University) and No. DE-SC0013847 (Vanderbilt University). C.J.H. is supported in part by U.S. DOE Grants No. DE-FG02-87ER40365 and No. DE-SC0018083. Z.L. gratefully acknowledges support from National Science Foundation under Grant No. PHY-1613708 (Arizona State University).

[1] I. Tanihata, H. Hamagaki, O. Hashimoto, Y. Shida, N. Yoshikawa, K. Sugimoto, O. Yamakawa, T. Kobayashi, and N. Takahashi, Phys. Rev. Lett. **55**, 2676 (1985).
[2] I. Tanihata *et al.*, Phys. Lett. B **160**, 380 (1985).
[3] A. Estradé *et al.*, Phys. Rev. Lett. **113**, 132501 (2014).
[4] S. Bagchi *et al.*, Phys. Lett. B **790**, 251 (2019).
[5] B. Blank *et al.*, Nucl. Phys. A **555**, 408 (1993).
[6] T. Kajino, W. Aoki, A. B. Balantekin, R. Diehl, M. A. Famiano, and G. J. Mathews, Prog. Part. Nucl. Phys. **107**, 109 (2019).
[7] Varinderjit Singh, J. Vadas, T. K. Steinbach, B. B. Wiggins, S. Hudan, R. T. deSouza, Zidu Lin, C. J. Horowitz, L. T. Baby, S. A. Kuvin, Vandana Tripathi, I. Wiedenhöver, and A. S. Umar, Phys. Lett. B **765**, 99 (2017).
[8] J. Vadas, V. Singh, B. B. Wiggins, J. Huston, S. Hudan, R. T. deSouza, Z. Lin, C. J. Horowitz, A. Chbihi, D. Ackermann, M. Famiano, and K. W. Brown, Phys. Rev. C **97**, 031601(R) (2018).
[9] C. J. Horowitz, H. Dussan, and D. K. Berry, Phys. Rev. C **77**, 045807 (2008).
[10] RIKEN, Nishina Center for Accelerator-Based Science, Japan.
[11] GANIL, Grand Accelérateur National d'Ions Lourds, Caen, France.
[12] NSCL, National Superconducting Cyclotron Laboratory, Michigan State University, USA.
[13] FRIB, Facility for Rare Isotope Beams, Michigan State University, USA.
[14] L. Canto, P. Gomes, J. Lubian, L. Chamon, and E. Crema, Nucl. Phys. A **821**, 51 (2009).
[15] A. V. Afanasjev, M. Beard, A. I. Chugunov, M. Wiescher, and D. G. Yakolev, Phys. Rev. C **85**, 054615 (2012).
[16] D. G. Kovar *et al.*, Phys. Rev. C **20**, 1305 (1979).
[17] Y. Eyal, M. Beckerman, R. Chechik, Z. Fraenkel, and H. Stocker, Phys. Rev. C **13**, 1527 (1976).
[18] B. Heusch, C. Beck, J. P. Coffin, P. Engelstein, R. M. Freeman, G. Guillaume, F. Haas, and P. Wagner, Phys. Rev. C **26**, 542 (1982).
[19] T. K. Steinbach, J. Vadas, J. Schmidt, C. Haycraft, S. Hudan, R. T. deSouza, L. T. Baby, S. A. Kuvin, I. Wiedenhöver, A. S. Umar, and V. E. Oberacker, Phys. Rev. C **90**, 041603(R) (2014).
[20] A. D. Frawley, N. R. Fletcher, and L. C. Dennis, Phys. Rev. C **25**, 860 (1982).
[21] J. Vadas, Probing the fusion of neutron-rich nuclei with modern radioactive beam facilities, Ph.D. thesis, Indiana University, 2018.
[22] L. R. Gasques, L. C. Chamon, D. Pereira, M. A. G. Alvarez, E. S. Rossi, C. P. Silva, and B. V. Carlson, Phys. Rev. C **69**, 034603 (2004).
[23] P. Ring, Prog. Part. Nucl. Phys. **37**, 193 (1996).
[24] B. D. Serot and J. D. Walecka, in *Advances in Nuclear Physics*, edited by J. W. Negele and E. Vogt (Plenum, New York, 1986), Vol. 16.

[25] M. Beard, A. V. Afanasjev, L. C. Chamon, L. R. Gasques, M. Wiescher, and D. G. Yakovlev, At. Data Nucl. Data Tables **96**, 541 (2010).
[26] D. G. Yakolev, M. Beard, L. R. Gasques, and M. Wiescher, Phys. Rev. C **82**, 044609 (2010).
[27] C. Y. Wong, Phys. Rev. Lett. **31**, 766 (1973).
[28] C. H. Dasso, S. Landowne, and A. Winther, Nucl. Phys. A **405**, 381 (1983).
[29] G. Montagnoli *et al.*, Phys. Rev. C **87**, 014611 (2013).
[30] K. Hagino, N. Rowley, and A. T. Kruppa, Comput. Phys. Commun. **123**, 143 (1999).
[31] O. Akyuz and A. Winther, in *Proceedings of the Enrico Fermi School of Physics 1979*, edited by R. A. Broglia, C. H. Dasso, and R. Ricci (North-Holland, Amsterdam, 1979).
[32] A. S. Umar and V. E. Oberacker, Phys. Rev. C **73**, 054607 (2006).
[33] A. S. Umar, V. E. Oberacker, and C. J. Horowitz, Phys. Rev. C **85**, 055801 (2012).
[34] R. T. deSouza, S. Hudan, V. E. Oberacker, and A. S. Umar, Phys. Rev. C **88**, 014602 (2013).
[35] A. S. Umar and V. E. Oberacker, Phys. Rev. C **74**, 021601(R) (2006).
[36] B. Blank, Z. Phys. A **343**, 375 (1992).
[37] A. Ozawa, T. Suzuki, and I. Tanihata, Nucl. Phys. A **693**, 32 (2001).
[38] W. Loveland, A. M. Vinodkumar, R. Yanez, L. Yao, J. King, J. Lassen, and A. Rojas, Eur. Phys. J. A **54**, 140 (2018).
[39] B. Paes, J. Lubian, P. R. S. Gomes, and V. Guimaräes, Nucl. Phys. A **890**, 1 (2012).
[40] T. Nakamura *et al.*, Phys. Lett. B **331**, 296 (1994).